

Studies of Surface Electrical Properties of Al doped ZnO Nanorods by STM

Shaivalini SINGH¹, Sumit VYAS², Parthasarathi CHAKRABARTI³, Si-Hyun PARK^{1*}

¹ Department of Electronic Engineering, Yeungnam University, 280 Daehak-ro, Gyeongsan-si, Gyeongsangbuk-do, 38541 Republic of Korea

² Department of Electronics and Communication Engineering, Thapar University, Patiala-147001, India

³ Department of Electronics Engineering, IIT BHU, Varanasi-221005, India

crossref <http://dx.doi.org/10.5755/j01.ms.23.2.15305>

Received 29 August 2016; accepted 03 October 2016

Pure and aluminum (Al) doped ZnO (Al:ZnO) nanorods (NRs) were deposited on silicon substrates by the hydrothermal method. The Al composition was kept at 2 % and 5 % for the Al:ZnO NR samples. The surface morphology and structural properties of the pure and Al:ZnO NRs were characterized by scanning electron microscopy (SEM) and X-ray diffraction (XRD), respectively. The XRD study revealed the hexagonal phase of the ZnO with (101), (002) and (100) peaks and it also revealed that the major orientation of ZnO NRs was along the (002) planes. The SEM micrographs showed perfectly grown ZnO NRs with hexagonal shaped tips. The electrical characterization of the pure and Al:ZnO NR thin film surface was done by scanning tunneling microscopy (STM). Local electron spectroscopy was conducted to measure the tunneling current with respect to the applied bias. The *n*-type behavior and bandgap of the pure and Al:ZnO NRs were confirmed from the $dI/dV - V$ characteristics. These studies are of fundamental importance for the fabrication of pure and Al:ZnO NR based nanodevices.

Keywords: hydrothermal, Al doped ZnO, nanorods, scanning tunnelling microscopy, X-ray diffraction.

1. INTRODUCTION

Among the various transparent conducting oxide (TCO) materials, ZnO is of particular interest [1, 2]. It is mainly used in photovoltaic cells, organic light-emitting diodes (OLEDs) and flat panel displays [3–5]. ZnO has a wide optical band gap (3.37 eV), high transparency in visible region, high exciton binding energy (60 meV) and very good conductivity [6]. The properties of ZnO like electrical conductivity, bandgap and transparency can be tuned and further improved by doping it with different impurities [1, 5–7]. Various nanostructures of pure ZnO and Al:ZnO are extensively used, because of their applications in nanogenerators [8], bio-sensors [9], UV-sensors [10], nanolasers [11] etc. Different kinds of nanostructures of pure ZnO and Al:ZnO are popular, including nanoparticles [12], nanowires [13], nanotubes [14], and nanorods (NRs) [15]. Al:ZnO NRs are one of the commonly used nanostructures for various devices [3–5]. These NRs can be grown by RF sputtering [16, 17], the sol-gel method [18], dip-coating [19], electrochemical deposition [20], the hydrothermal method [21], and chemical vapor deposition [22], etc. In this work, we used the hydrothermal method for the growth of the Al:ZnO NRs.

In order to fabricate Al:ZnO NR based devices, a detailed study of their surface and electronic properties is necessary. In this work, we studied the electronic properties of Al:ZnO NR films using scanning tunneling microscopy (STM). Previously, STM was used to study various semiconductors, such as ZnS, SnS₂ and graphene [23–25]. Few research groups have also reported the STM

studies of Al:ZnO thin films deposited by RF-sputtering [26, 27]. However, till now, no any research group has reported STM studies of Al:ZnO NRs grown by hydrothermal method. In this work, we have systematically examined the structural and electrical properties of pure and Al:ZnO NRs. The characteristics of the pure and Al:ZnO NRs samples were investigated by X-ray diffraction (XRD), scanning electron microscopy (SEM) and STM respectively.

2. EXPERIMENTAL TECHNIQUE

NR thin films of pure and Al:ZnO were grown on *p*-type silicon wafers. All of the wafers were cleaned in acetone and methanol for 10 min using an ultrasonic bath and then washed with deionized (DI) water. The NRs were grown on Si wafers in two steps. Firstly, a seed layer of pure ZnO is deposited on the Si wafer. Then, pure and Al:ZnO NR thin films were grown in the second step, on the previously grown seed layer. Zinc acetate dihydrate powder and ethyl alcohol were used as precursors for the growth of the seed layer. The concentration of seed layer solution was 60 mM and the solution was mixed for one hour at 80 °C temperature [28]. Zinc nitrate hexahydrate (ZN), hexa-methylene-tetramine (HMT) and DI water were used as precursors for the growth of the pure ZnO NRs. The concentration of main-growth solution was 30 mM [29]. Aluminum nitrate nonahydrate, ZN, HMT and DI water were used as precursors for the growth of the Al doped ZnO NRs. For preparing Al doped ZnO NRs samples, 2 wt.% and 5 wt.% aluminum nitrate nonahydrate was mixed with ZN, HMT and DI water. The more detail and the principle experimental scheme of the hydrothermal growth setup can be found in the elsewhere [30].

* Corresponding author. Tel.: +82-53-810-3096.

E-mail address: sihyun_park@ynu.ac.kr (S.-H. Park)

3. CHARACTERIZATION

The structure of the pure and Al:ZnO NRs was studied using XRD (PAN Analytical X'PERT PRO XRD system with Cu K α radiation ($\lambda = 1.540568 \text{ \AA}$). The surface morphology of the pure and Al:ZnO NRs was characterized by SEM (HITACHI S-4800, Japan).

The I - V characteristics of the surface of pure ZnO and Al:ZnO NR thin films were measured with nanoREV Ambient Air STM system (from Quazar Technologies Pvt. Ltd.). The schematic diagram of STM set-up is shown in the Fig. 1. The STM experiment was done with the tip of Platinum-Iridium. The electrical continuity was maintained during the experiment. A small piece of silver (Ag) paste was used to ground the bottom metallic plate and the surface of ZnO NR thin films. The I - V characteristics were measured at already selected places, during the scanning. When the tip reached at that particular locations, the feedback loop was stopped for a while and the current reading was saved. The sample voltage was increased linearly from -5V to $+5\text{V}$ in very less time interval (~ 100 milli second). The measurement was repeated after a small interval of time. Multiple readings has been taken for each location and with the average of all those reading the resultant curves were obtained.

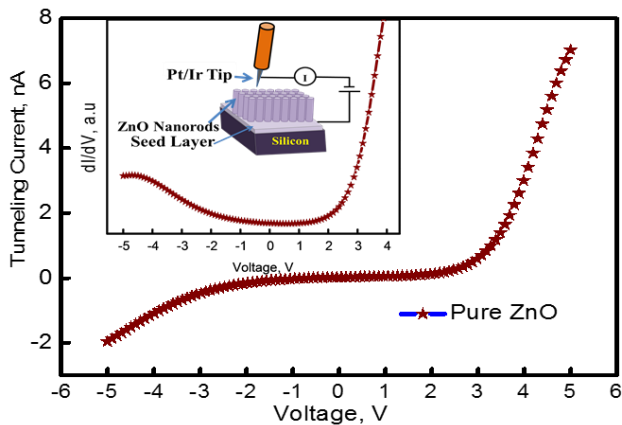


Fig. 1. Scheme of measurement set-up for STM (inset-2); I - V and dI/dV - V (inset-1) characteristics of pure ZnO NR samples measured from STM

4. RESULTS AND DISCUSSION

Fig. 2 a–c shows the XRD patterns of the pure and 2 %, 5 % Al:ZnO NRs grown on p -Si substrates respectively. It shows a wurtzite structure with hexagonal phase and space group, P63mc [31].

The growth of NRs are along (101), (002) and (101) direction, but, the main XRD peak for the pure and Al:ZnO NRs corresponding to the (002) orientation. For 5 % Al doped ZnO, there is also a small peak around 48° , that corresponds to orientation along (102) planes. This means that higher Al concentrations degrade the crystalline structure of ZnO NRs. There is no any trace of any other diffraction peaks, such as for $\text{Zn}_{(1-x)}\text{Al}_x\text{O}_4$, ZnAl_2O_4 or Al_2O_3 . This confirms that all of the Al^{3+} has been successfully substituted for the Zn^{2+} sites within the ZnO lattice [32]. Fig. 3 shows the SEM micrographs of the pure and 2 % and 5 % Al:ZnO NRs.

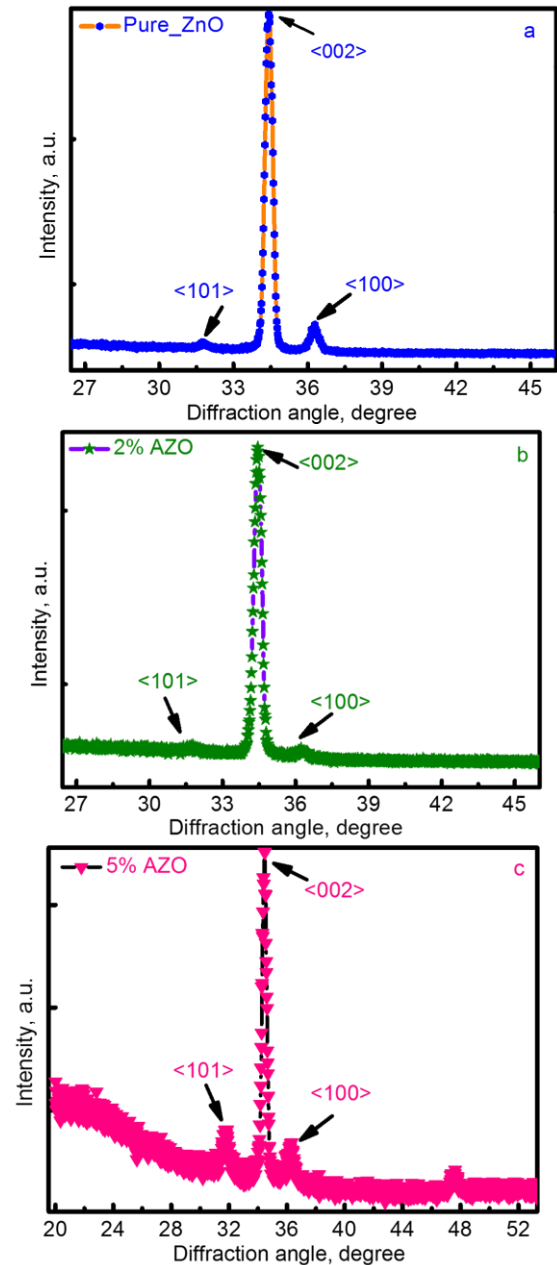


Fig. 2. XRD spectra: a–Pure ZnO NRs; b–2 % Al:ZnO NRs; c–5 % Al:ZnO, grown by hydrothermal method

It can be seen that the pure and Al:ZnO NRs were successfully grown as vertical-rod like structures with a hexagonal shaped rod-tip. The radius of the tip of the NRs was measured from the SEM images and found to be in the range of 20 to 25 nm. The growth of the NRs was uniform and their density increases with the increase in Al doping concentration from 0 % (pure) to 5 % [33].

To study the effect of Al doping on the electrical characteristics of the surface of the pure and Al:ZnO NRs, STM-measurements were performed. A schematic diagram of the STM set-up is shown in the inset of Fig. 1. The voltage was applied in the range of $\pm 5\text{V}$ and the tunneling current values were plotted as shown in Fig. 1 and Fig. 4. It can be seen from the graphs that the I - V characteristics are rectifying in nature [34]. This kind of I - V characteristics is mainly due to formation of Schottky contact between the ZnO and the metal (Pt/Ir) of STM-tip. Earlier Schottky-

Mott has given one theory, which states that if the electron affinity (EA) of a semiconductor will be smaller than the work function (WF) of the metal, Schottky-contact will be formed [35]. Hence, in our case, the Pt/Ir and ZnO NRs form a Schottky contact, which gives rise to a nonlinear tunneling current [36]. For Al:ZnO, the I - V characteristics is less rectifying as compared to ZnO NRs. This can be attributed to the increase in conductivity of ZnO by Al doping.

The STM-conductance characteristics for the Pt/Ir and NRs were also measured, as shown in the insets of Fig. 3 and Fig. 4, respectively. The position $V = 0$ in the dI/dV vs. V graph corresponds to the Fermi level, whereas the left and right sides with respect to $V = 0$, correspond to the valence-band and conduction-band energy-levels of the semiconductor, respectively [26].

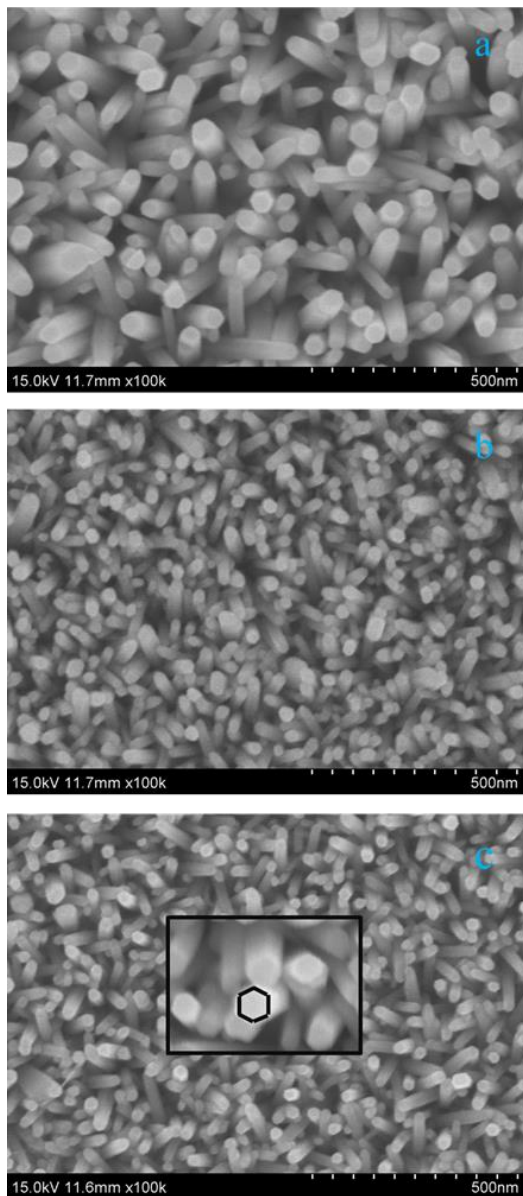


Fig. 3. High-resolution micrograph showing hexagonal-tip of nanorods (inset); SEM image: a – pure ZnO NRs; b – 2 % Al:ZnO NRs; c – 5 % Al:ZnO, grown by hydrothermal method

The dI/dV vs. V graphs in the insets of Fig. 1 and Fig. 4 show that the position of the conduction band is nearer to the Fermi level, which confirms the n -type nature of the ZnO. The dI/dV vs. V graphs for 2 % ZnO NR samples shows that the Fermi level is closer to conduction band as compared to Fermi level in ZnO NR samples. The dI/dV vs. V graphs for 5 % ZnO NR samples reveals that the Fermi level is less closer to conduction band as compared to Fermi level in 2 % Al:ZnO, but it is more closer as compared to pure ZnO NR. These dI/dV vs. V graphs were also investigated for the purpose of measuring the bandgap of the undoped and 2 % and 5 % Al:ZnO NR samples. The bandgaps of the pure and 2 % and 5 % Al:ZnO NR surfaces were estimated to be 3.22 eV, 3.28 eV and 3.25 eV. The increase in the bandgap of 2 % Al:ZnO as compared to undoped ZnO NRs may be due to Burstein-Moss (B-M) effect. The decrease in bandgap of 5 % Al:ZnO and as compared to 2 % Al:ZnO may be attributed to bandgap narrowing which occurs because of heavy doping.

The thicknesses of the pure and Al:ZnO NR samples were measured by cross-sectional SEM (not shown here) and found to be ~ 800 – 900 nm, ~ 300 – 400 nm and ~ 350 – 400 nm for the pure ZnO NR and 2 % and 5 % Al:ZnO NR samples, respectively. It is noticed that the height of the nanorods were different for pure ZnO and Al:ZnO. It can be understood by the facts that the doping of Al causes reduction in the growth-rate of nanorods. The doping of ZnO lattice was attained by substitution reaction. The atomic radius of Zn and Al are 1.35 Å and 1.25 Å respectively. Probably this difference in the radius causes the difference in the heights of pure ZnO and Al: ZnO nanorods [27].

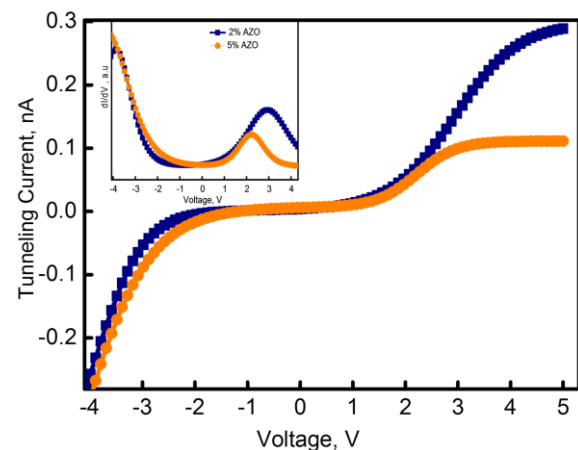


Fig. 4. I - V and dI/dV - V (inset) characteristics of 2 % and 5 % Al:ZnO NRs samples measured from STM

4. CONCLUSIONS

Pure ZnO and 2% and 5% Al:ZnO thin films were grown by the hydrothermal method and their structural and electrical properties were investigated by XRD, SEM, and STM measurements. The XRD patterns of the pure and Al:ZnO NRs showed a strong peak for the $\langle 002 \rangle$ orientation but the crystalline nature of ZnO was affected with the increase in Al concentration. The SEM images of all of the NR films showed that their surface was smooth

and uniform and density of NRs were found to increase with the increase in Al concentration. The electrical properties of the surface of the pure and Al:ZnO NRs were investigated by STM, and the tunneling current was obtained by applying voltage biases in the range of - 5 V to + 5 V. The I - V characteristics of the pure and Al:ZnO NRs showed non-linear behavior and the STM conductance spectra were also obtained from the dI/dV vs. V curve. With the help of conductance spectra, the bandgap of pure and Al:ZnO NRs were measured and the bandgap was found to be altered with the incorporation and change in the Al concentration.

Acknowledgments

The authors gratefully acknowledge the facilities provided by the Centre for Interdisciplinary Research (CIR) of the institute M.N.N.I.T Allahabad.

REFERENCES

1. **Minami, T.** Transparent conducting oxide semiconductors for transparent electrodes *Semiconductor Science and Technology* 20 2005: pp. S35–S44. <https://doi.org/10.1088/0268-1242/20/4/004>
2. **Stadler, A.** Transparent conducting oxides – An up-to-date overview *Materials* 5 2012: pp. 661–683. <https://doi.org/10.3390/ma5040661>
3. **Lungu, J., Georgescu, A., Dumbrava, A.** Enhancing the efficiency of AZO-based dye sensitized solar cells by surface treatments *Scientific Study & Research* 16 2015: pp. 069–074.
4. **Li, F., Zhang, Y., Wu, C., Lin, Z., Zhang, B., Guo, T.** Improving efficiency of organic light-emitting diodes fabricated utilizing AZO/Ag/AZO multilayer electrode *Vacuum* 86 2012: pp. 1895–1897. <https://doi.org/10.1016/j.vacuum.2012.05.028>
5. **Liu, Y., Li, Y., Zeng, H.** ZnO-based transparent conductive thin films: doping, performance, and processing *Journal of Nanomaterials* 2013 2013: pp. 1–8.
6. **Wang, Z.L.** Zinc oxide nanostructures: growth, properties and applications *Journal of Physics: Condensed Matter* 16 2004: pp. R829–R858. <https://doi.org/10.1088/0953-8984/16/25/R01>
7. **Jung, K., Shin, D.W., Yoon, S.J., Choi, J.W., Choi, W.K., Song, J.H., Kim, H.J.** Electrical and optical properties of Al-doped zinc-oxide thin films deposited at room temperature by using the continuous composition spread method *Journal of the Korean Physical Society* 57 2010: pp. 1092–1095. <https://doi.org/10.3938/jkps.57.1092>
8. **Wang, Z.L.** From nanogenerators to piezotronics – A decade-long study of ZnO nanostructures *MRS Bulletin* 37 2012: pp. 814–827. <https://doi.org/10.1557/mrs.2012.186>
9. **Bajpai, R., Zaghoul, M., Gu, D., Baumgart, H., Abdel-Fattah, T.M.** Synthesis and assembly of ZnO nanorods grown by ALD for biosensor application *Semiconductor Device Research Symposium ISDRS '09, 2009: International, College Park, MD*, pp. 1-2.
10. **Gedamu, D., Paulowicz, I., Kaps, S., Lupan, O., Wille, S., Haidarschin, G., Mishra, Y.K., Adelung, R.** Rapid fabrication technique for interpenetrated ZnO nanotetrapod networks for fast UV Sensors *Advanced Materials* 26 2014: pp. 1541–1550. <https://doi.org/10.1002/adma.201304363>
11. **Chou, Y.H., Chou, B.T., Chiang, C.K., Lai, Y.Y., Yang, C.T., Li, H., Lin, T.R., Lin, C.C., Kuo, H.C., Wang, S.C., Lu, T.C.** Ultrastrong mode confinement in ZnO surface plasmon nanolasers *ACS Nano* 9 2015: pp. 3978–3983. <https://doi.org/10.1021/acs.nano.5b01643>
12. **Stypula, B., Kmita, A., Hajos, M.** Morphology and Structure of ZnO Nanoparticles Produced by Electrochemical Method *Materials Science (Medžiagotyra)* 20 2014: pp. 3–9.
13. **Yang, X., Shan, C.X., Jiang, M.M., Qin, J.M., Hu, G.C., Wang, S.P., Ma, H.A., Jia, X.P., Shen, D.Z.** Intense electroluminescence from ZnO nanowires *Journal of Materials Chemistry C* 3 2015: pp. 5292–5296. <https://doi.org/10.1039/C5TC00317B>
14. **Fuxue, W., Xiaolong, C., Dawei, Y., Zhaomin, Z., Shaoqing, X., Xiaofeng, G.** Synthesis and luminescence characteristics of ZnO nanotubes *Journal of Semiconductors* 35 2014: 093004 (1–5).
15. **Sonmez, E., Meral, K.** Enhancement of photoluminescence lifetime of ZnO nanorods making use of thiourea *Journal of Nanomaterials* 2012 2012: pp. 1–6.
16. **Venkatesh, P.S., Dong, C.L., Chen, C.L., Pong, W.F., Asokan, K., Jeganathan, K.** Local electronic structure of ZnO nanorods grown by radio frequency magnetron sputtering *Materials Letters* 116 2014: pp. 206–208. <https://doi.org/10.1016/j.matlet.2013.11.034>
17. **Her, S.C., Chi, T.C.** Optical and electrical performance of ZnO films textured by chemical etching *Materials Science (Medžiagotyra)* 21 2015: pp. 502–505.
18. **Foo, K.L., Hashim, U., Muhammad, K., Voon, C.H.** Sol–gel synthesized zinc oxide nanorods and their structural and optical investigation for optoelectronic application *Nanoscale Research Letters* 9 2014: pp. 1–10. <https://doi.org/10.1186/1556-276X-9-429>
19. **Schmack, R., Eckhardt, B., Koch, G., Ortel, E., Kraehnert, R.** ZnO coatings with controlled pore size, crystallinity and electrical conductivity *Materials Science (Medžiagotyra)* 22 2016: pp. 74–81.
20. **Šulčiūtė, A., Valatka, E.** Electrodeposition and photoelectrocatalytic activity of ZnO films on AISI 304 type steel *Materials Science (Medžiagotyra)* 18 2012: pp. 318–324.
21. **Schlur, L., Carton, A., Lévêque, P., Guillon, D., Pourroy, G.** Optimization of a New ZnO Nanorods hydrothermal synthesis method for solid state dye sensitized solar cells applications *Journal of Physical Chemistry C* 117 2013: pp. 2993–3001. <https://doi.org/10.1021/jp305787r>
22. **Zhao, R.R., Wei, X.Q., Ding, M., Xu, X.J.** Fabrication and Optical Properties of Mg-Doped ZnO Nanorods by Chemical Vapor Deposition *Science of Advanced Materials* 6 2014: pp. 500–504.
23. **Thupakula, U., Bal, J.K., Dalui, A., Debangshi, A., Sarma, D.D., Acharya, S.** Current rectification by a single ZnS nanorod probed using a scanning tunneling microscopic technique *Journal of Materials Chemistry C* 2 2014: pp. 1158–1164. <https://doi.org/10.1039/c3tc31850h>
24. **Etefagh, R., Shahtahmasebi, N., Karimipour, M.** Effect of Zn doping on optical properties and photoconductivity of SnS₂ nanocrystalline thin films *Bulletin Material Science* 36 2013: pp. 411–416.

<https://doi.org/10.1007/s12034-013-0481-0>

25. **Phark, S.H., Borme, J., Vanegas, A.L., Corbetta, M., Sander, D., Kirschner, J.** Scanning tunneling spectroscopy of epitaxial graphene nanoisland on Ir(111) *Nanoscale Research Letters* 7 2012: pp. 1–4.
<https://doi.org/10.1186/1556-276X-7-255>
26. **Likovich, E.M., Jaramillo, R., Russell, K.J., Ramanathan, S., Narayanamurti, V.** Narrow Band Defect Luminescence from Al-doped ZnO Probed by Scanning Tunneling Cathodoluminescence *Applied Physics Letter* 99 2011: pp. 151910 (1–3).
27. **Likovich, E.M., Jaramillo, R., Russell, K.J., Ramanathan, S., Narayanamurti, V.** Scanning tunneling microscope investigation of local density of states in Al-doped ZnO thin films *Physical Review B* 83 2011: pp. 075430 (1–6).
28. **Singh, S., Park, S.H.** Low temperature hydrothermal growth of zno nanorod films for schottky diode application *Korean Journal of Metals and Materials* 54 2016: pp. 347–351.
29. **Nam, G.H., Baek, S.H., Park, I.K.** Growth of ZnO nanorods on graphite substrate and its application for Schottky diode *Journal of Alloys and Compounds* 613 2014: pp. 37–41.
<https://doi.org/10.1016/j.jallcom.2014.05.110>
30. **Xu, S., Wang, Z.L.** One-dimensional ZnO nanostructures: solution growth and functional properties *Nano Research* 4 2011: pp. 1013–1098.
<https://doi.org/10.1007/s12274-011-0160-7>
31. **Lim, S.K., Hong, S.H., Hwang, S.H., Choi, W.M., Kim, S., Park, H., Jeong, M.G.** Synthesis of Al-doped ZnO nanorods via Microemulsion method and their application as a CO gas sensor *Journal of Materials Science & Technology* 31 2015: pp. 639–644.
<https://doi.org/10.1016/j.jmst.2014.12.004>
32. **Dasgupta, N.P., Neubert, S., Lee, W., Trejo, O., Lee, J.R., Prinz, F.B.** Atomic layer deposition of Al-doped ZnO films: effect of grain orientation on conductivity *Chemistry of Materials* 22 2010: pp. 4769–4775.
<https://doi.org/10.1021/cm101227h>
33. **Lu, Y.M., Tang, J.F.** Electro-optical and structural properties of Al-doped ZnO nanorod arrays prepared by hydrothermal process *International Journal of Science and Engineering* 3 2013: pp. 11–15.
34. **Brillson, L.J., Lu, Y.** ZnO Schottky barriers and Ohmic contacts *Journal of Applied Physics* 109 2011: pp. 121301 (1–33).
35. **Zeng, Y.J., Schouteden, K., Amini, M.N., Ruan, S.C., Lu, Y.F., Ye, Z.Z., Partoens, B., Lamoen, D., Haesendonck, C.V.** Electronic band structures and native point defects of ultrafine zno nanocrystals *ACS Applied Materials & Interfaces* 7 2015: pp. 10617–10622.
<https://doi.org/10.1021/acsami.5b02545>
36. **Stavale, F., Pascua, L., Nilus, N., Freund, H.J.** Morphology and luminescence of ZnO films grown on a Au(111) support *Journal of Physical Chemistry C* 117 2013: pp. 10552–10557.
<https://doi.org/10.1021/jp401939x>